Published in final edited form as:
Am J Physiol Heart Circ Physiol. 2007 July ; 293(1): H610–H619.

Cannabidiol attenuates high glucose-induced endothelial cell inflammatory response and barrier disruption

Mohanraj Rajesh[1], **Partha Mukhopadhyay**[1], **Sándor Bátkai**[1], **György Haskó**[2], **Lucas Liaudet**[3], **Viktor R. Drel**[4], **Irina G. Obrosova**[4], and **Pál Pacher**[1]

[1]*Laboratory of Physiological Studies, National Institute on Alcohol Abuse and Alcoholism, National Institutes of Health, Bethesda, Maryland* [2]*Department of Surgery, University of Medicine and Dentistry of New Jersey-New Jersey Medical School, Newark, New Jersey* [3]*Department of Intensive Care Medicine, University Hospital, Lausanne, Switzerland* [4]*Pennington Biomedical Research Center, Louisiana State University System, Baton Rouge, Louisiana*

Abstract

A nonpsychoactive cannabinoid cannabidiol (CBD) has been shown to exert potent anti-inflammatory and antioxidant effects and has recently been reported to lower the incidence of diabetes in nonobese diabetic mice and to preserve the blood-retinal barrier in experimental diabetes. In this study we have investigated the effects of CBD on high glucose (HG)-induced, mitochondrial superoxide generation, NF-κB activation, nitrotyrosine formation, inducible nitric oxide synthase (iNOS) and adhesion molecules ICAM-1 and VCAM-1 expression, monocyte-endothelial adhesion, transendothelial migration of monocytes, and disruption of endothelial barrier function in human coronary artery endothelial cells (HCAECs). HG markedly increased mitochondrial superoxide generation (measured by flow cytometry using MitoSOX), NF-κB activation, nitrotyrosine formation, upregulation of iNOS and adhesion molecules ICAM-1 and VCAM-1, transendothelial migration of monocytes, and monocyte-endothelial adhesion in HCAECs. HG also decreased endothelial barrier function measured by increased permeability and diminished expression of vascular endothelial cadherin in HCAECs. Remarkably, all the above mentioned effects of HG were attenuated by CBD pretreatment. Since a disruption of the endothelial function and integrity by HG is a crucial early event underlying the development of various diabetic complications, our results suggest that CBD, which has recently been approved for the treatment of inflammation, pain, and spasticity associated with multiple sclerosis in humans, may have significant therapeutic benefits against diabetic complications and atherosclerosis.

Keywords

oxidative stress; peroxynitrite; cannabinoids; endocannabinoids; inflammation; atherosclerosis

The majority of diabetic complications are associated with pathophysiological alterations in the vasculature. Micro- and macrovascular diseases are the most common causes of morbidity and mortality in patients with diabetes mellitus. Microvascular complications involve retinopathy and nephropathy, the leading causes of blindness and renal failure. Atherosclerosis is the most common macrovascular complication of diabetes, which increases the risk for stroke, myocardial infarction, and peripheral artery disease, the latter being the leading cause of limb amputation in civilized countries. Hyperglycemia has been implicated in the activation

Address for reprint requests and other correspondence: P. Pacher, Section on Oxidative Stress Tissue Injury, Laboratory of Physiological Studies, National Institutes of Health/NIAAA, 5625 Fishers Ln., MSC-9413, Bethesda, MD 20892-9413 (e-mail: pacher@mail.nih.gov).

of numerous key mechanisms/pathways including oxidative (5,50) and nitrosative stress (38, 41,50), advanced glycation end products (4), aldose reductase (23,35), protein kinase C (24), and nuclear enzyme poly(ADP-ribose) polymerase (3,39,42,51), which in concert result in endothelial dysfunction in diabetic blood vessels underlying the development of various diabetic complications. One of the key early events in the pathogenesis of atherosclerosis is the adhesion of monocytes to the endothelium followed by transmigration into the subendothelial space (16,17). Studies have demonstrated increased leukocyte-endothelial interactions with monocytes from diabetic patients (16,29), in animal models of diabetes (16, 54), and also in cells exposed to high glucose (HG) in vitro (13,27,49,52). Importantly, the hyperglycemia/HG-induced augmentation of leukocyte adhesion to the endothelium through upregulation of cell surface expression of adhesion molecules and transendothelial migration (TEM) has been reported to be dependent on NF-κB activation (21,32).

Cannabinoids, components of the *Cannabis sativa* (marijuana) plant, are known to exert potent anti-inflammatory, immunomodulatory and analgesic effects through activation of cannabinoid-1 and -2 (CB_1 and CB_2) receptors located in the central nervous system and immune cells (28,37). The limitation of the therapeutic utility of the major cannabinoid, Δ^9-tetrahydrocannabinol, is the development of psychoactive effects through central nervous system CB_1 receptor (37). In contrast, cannabidiol (CBD), one of the most abundant cannabinoids of *Cannabis sativa* with reported antioxidant, anti-inflammatory, and immunomodulatory effects is well tolerated without side effects when chronically administered to humans (7,11) and is devoid of psychoactive properties due to a low affinity for the CB_1 and CB_2 receptors (37,53).

Here we have studied the effects of CBD on HG-induced mitochondrial superoxide generation, NF-κB activation, inducible nitric oxide synthase (iNOS) expression, nitrotyrosine formation [footprint of peroxynitrite generation (38)], upregulation of adhesion molecules ICAM-1 and VCAM-1, monocyte-endothelial adhesion, TEM of monocytes, and disruption of endothelial barrier function in human coronary artery endothelial cells (HCAECs). Our results may have important relevance for the prevention/treatment of diabetic complications and atherosclerosis.

MATERIALS AND METHODS

Reagents

1-(2,4-Dichlorophenyl)-5-(4-iodophenyl)-4-methyl-*N*-4-moepholinyl-1*H*-pyrazole-3-carboxamide (AM 281) and 6-iodo-2-methyl-1-[2-(4-morpholinyl)ethyl]-1*H*-indol-3-yl](4-methoxyphenyl) methanone (AM 630) were purchased from Tocris Bioscience (Ellisville, MO). *N*-piperidino-5-(4-chlorophenyl)-1-(2,4-dichloro-phenyl)-4-methyl-3-pyrazole-carboxamide (SR 141716A; designated as SR1) and {*N*-[1*S*]-endo-1,3,3-trimethylbicyclo [2.2.1]heptan-2-yl]-5-(4-chloro-3-methylphenyl)-1-(4-methylbenzyl)-pyrazole-3-carboxamide} (SR 144528; designated as SR 2) was from Research Triangle Institute (Research Triangle Park, NC). CBD was obtained from either Tocris Bioscience or isolated from hashish as described earlier (15). Sources of all the other reagents used in the experiments are mentioned in the text wherever appropriate.

Cell culture

HCAECs and growth medium were purchased from Cell Applications (San Diego, CA). HCAECs were grown in HCAEC growth medium in cell culture dishes coated with 0.2% gelatin. HCAECs were used for the experiments between *passages 3–7*. Human monocytic cell line (THP-1) was obtained from American Type Culture Collection and was grown in RPMI 1640 medium supplemented with 2 mM L-glutamine, 10 mM HEPES, 10% fetal bovine

serum, 100 U/ml penicillin, and 100 μg/ml streptomycin (Invitrogen, CA). The cells were maintained at 37°C in an incubator containing 5% CO_2-95% room air.

Cell surface ICAM-1 and VCAM-1 expression assay

Cell surface expression of ICAM-1 and VCAM-1 was measured using in situ ELISA as described (2). In brief, HCAECs were grown in 96-well plates coated with 0.2% gelatin. The cells were treated with either 5 or 30 mM D-glucose (designated as HG) alone for 48 h (33). In some experiments, cells were pretreated with either specific CB_1 antagonists SR1/AM 281 or CB_2 antagonists SR2/AM 630 for 1 h, followed by continued incubation with HG ± CBD for 48 h.

Western immunoblot analysis of ICAM-1 and VCAM-1 expression

After treatment, cells were washed two times with PBS, and total cell lysate was prepared using radioimmunoprecipitation assay lysis buffer (Pierce Biotechnology) supplemented with cocktail of protease inhibitors (Roche). Protein (25 μg) was resolved in 12% SDS-PAGE and probed with either mouse anti-human ICAM-1/VCAM-1 (1:1,000, R&D systems), and the blots were incubated overnight at 4°C. After being washed, the blots were incubated with secondary antibody goat anti-mouse horseradish peroxidase (Pierce, 1:5,000) for 1 h at room temperature (RT). The blots were then developed with SuperSignal enhanced chemiluminescent substrate solution (Pierce). To verify equal loading, blots were stripped (Pierce) and reprobed with β-actin (Chemicon).

Monocyte adhesion assay

The determination of monocyte adhesion to the endothelial cells was conducted using human THP-1 cells as described (27). In brief, HCAECs were grown to confluence in 24-well plates and treated with HG/CBD ± CB_1/CB_2 antagonists. THP-1 cells were labeled with 1.5 μM calcein-AM (Molecular Probes; Invitrogen, CA) for 1 h at 37°C in RPMI 1640 containing 1% FBS. Labeled THP-1 cells (10^5/100 μl) were then added to HCAECs and incubated for 1 h at 37°C in an incubator containing 5% CO_2-95% room air. After incubation, the medium containing monocytes was aspirated and the monolayer was gently washed with PBS three times to remove the unbound monocytes. The adherent monocytes were documented using an Olympus IX 81 fluorescent microscope using a × 10 objective with a × 1.5 digital zoom. Three fields were captured per experimental condition. Individual treatments were performed in duplicates, and the entire set of experiments was repeated at least three times. The number of adherent THP-1 cells was counted using National Institutes of Health ImageJ software, and the values were expressed as adhered cells per field.

Monocyte TEM assay

HCAECs were grown to confluence on 0.2% gelatin-coated 3.0-μm polyethylene terepthalate track-etched cell culture inserts (BD Biosciences). The assays were performed essentially as described with minor modifications to the protocol (44). Confluent HCAECs were treated with HG/CDB ± CB_1/CB_2 antagonists as mentioned in the aforementioned experiments. THP-1 cells were then labeled with 2 μM Cell Tracker Green 5-chloromethylfluorescein diacetate (CMDFA, Molecular Probes) according to the protocol supplied by the manufacturer. Labeled THP-1 cells (3×10^5/200 μl) were added to the upper compartment of the cell culture insert, and the lower compartment of the insert contained 0.5 ml of RPMI 1640. Subsequently, the monocytes were allowed to transmigrate for 4 h at 37°C in an environment of 5% CO_2-95% room air. Finally, the culture inserts were removed, and the fluorescence in the lower chamber was measured using the Victor-Wallac Multilabel counter (Perkin Elmer) with excitation at 492 nm and emission at 571 nm. The fluorescence of the lower chamber was proportional to

the number of monocytes that were transmigrated. The monocyte TEM was expressed as a percentage, and the set of experiments was repeated independently three times.

Immunofluorescece staining for vascular endothelial cadherin expression

HCAECs were grown to confluence in glass chamber slides (Lab-Tek, Nalgene Nunc) and treated with HG alone or pretreated with CBD for 1 h followed by incubation with HG for 48 h. After the incubation, cells were fixed in 4% paraformaldehyde for 20 min at RT. Subsequently, the cells were permiabilized with 0.2% Triton X-100 for 20 min at RT. After being washed with PBS, the cells were incubated with anti-human vascular endothelial cadherin (VE-cadherin) antibody (1:150; mouse monoclonal, R&D Systems) for 5 h at 4°C. In the subsequent step, the cells were probed with goat anti-mouse FITC conjugate (1:250, Pierce) for 1 h at RT. The nucleus was counterstained with propidium iodide (Molecular Probes). Images were obtained using a fluorescent microscope (Olympus IX 81) at a ×20 objective with a ×1.5 digital zoom.

In vitro vascular permeability assay

HCAECs were grown to confluence in polycarbonate cell culture inserts (0.4 μm pore size, 6.5 mm diameter) in 24-well companion plates (BD Biosciences). The assays were performed as described earlier (48). The growth medium was removed and replaced with 100 μl of 2% FBS growth factor free medium (upper chamber) and 0.5 ml in the lower chamber. Cells were pretreated with either CBD or CB_1/CB_2 antagonists for 1 h and continued incubation with HG for 48 h. Subsequently, the medium was removed and replaced with 100 μl of serum and growth factor free medium (upper chamber) containing FITC-dextran (40 kDa, Molecular Probes). This step was followed by incubation of the inserts at 37°C in an environment of 5% CO_2-95% room air for 45 min. The fluorescence intensities of the solution in the lower chamber were measured using Victor-Wallac Multilabel Counter System (Perkin Elmer) with excitation at 485 nm and emission at 535 nm.

Analysis of NF-κB activation

NF-κB activation was analyzed by measuring inhibitory κB-α factor (IκB-α) degradation and subsequent translocation of NF-κB (p65) to the nucleus using Western blot assays. HCAECs were grown to confluence in 100 mm cell culture dishes. The cells were then treated with either HG or CBD alone for 48 h or pretreated with CB_1/CB_2 antagonists followed by incubation with HG and/or CBD for 48 h. Subsequently, nuclear and cytoplasmic extracts were prepared using mammalian nuclear protein extraction reagent (NPER; Pierce) by following the manufacturer's instructions. Nuclear protein (30 μg) or cytoplasmic extracts (20 μg) were resolved on a 12% SDS-PAGE and then transferred to nitrocellulose membrane. After being blocked, the membranes were probed with human anti-IκB-α (rabbit monoclonal, Cell Signaling Technology) in the case of cytoplasmic extract or with anti-human NF-κB (p65) (mouse monoclonal, Invitrogen) in the case of the nuclear extract blots at 1:1,000 and 1:1,500 dilutions, respectively, and incubated overnight at 4°C. Subsequently, the membranes were washed and incubated with appropriate secondary antibodies for 1 h at RT. Finally, the bands were visualized using West Pico chemiluminescence substrate reagent (Pierce). The protein concentration in the cellular extracts was measured using the Bio-Rad Lowry assay kit. The band densities were determined using Image Quant software (Molecular Devices). IκB-α degradation was expressed as the ratio of IκB-α to β-Actin, whereas the NF-κB expression was denoted by percent increase after normalizing the NF-κB expression with histone 2B as the loading control. Furthermore, HG-induced NF-κB activation was also confirmed by using immunoflourescene assay, indicating the nuclear translocation of NF-κB.

Determination of mitochondrial superoxide generation

HCAECs were seeded in 0.2% gelatin-coated 12-well culture dishes and allowed to reach confluence. The cells were then preconditioned in growth factor free medium containing 2% FBS for 4 h, followed by treatments with 5 mM glucose, 30 mM HG, and 30 mM D-mannitol for 48 h. In some experiments, cells were incubated with CBD (4 μM) alone for 48 h, or added 1 h before, the treatment with HG and incubated for 48 h. At the end of incubation, MitoSOX red (5.0 μM; Molecular Probes/Invitrogen) was added to the cells and incubated further for 15 min at 37°C in an atmosphere of 5% CO_2-95% room air as described (43,45). Subsequently, cells were collected by trypsinization and washed in PBS supplemented with 1% BSA, and measurements were performed using FACS caliber system (BD Biosciences). MitoSOX red was excited by laser at 488 nm, and the data were collected at 585/42 nm (FL2) channel. The data were presented by histogram of mean intensity of MitoSOX fluorescence.

iNOS expression and 3-nitrotyrosine accumulation

HCAECs were treated with normal glucose, CBD (4 μM), or HG alone for 48 h or pretreated with CBD for 1 h followed by treatment with HG for 48 h. After incubation, iNOS expression [anti-human iNOS (mouse monoclonal) BD Biosciences] and 3-nitrotyrosine (3-NT) formation (rabbit polyclonal, Cayman Chemicals) were analyzed by Western blot analysis and immunofluorescence staining.

Statistical analysis

All values are represented as means ± SE. Statistical significance of the data was assessed by paired Student's *t*-test or one-way ANOVA as appropriate. $P < 0.05$ was considered significant.

RESULTS

CBD inhibits HG-induced upregulation of ICAM-1 and VCAM-1

HG treatment of HCAECs resulted in a marked upregulation of ICAM-1 (Fig. 1*A*) and VCAM-1 (Fig. 1*B*) expression by ~6.0- and 5.5-fold, respectively, when compared with normal glucose-treated cells. This upregulation of ICAM-1 and VCAM-1 expression was dose-dependently reduced by CBD (0–6 μM) pretreatment (Fig. 1, *A* and *B*). The effect of CBD was not preventable by either CB_1 or CB_2 antagonists, which by themselves had no effect on HG-induced increased adhesion molecule expression (Fig. 1, *C* and *D*). L-Glucose (30 mM) or D-mannitol (30 mM) had no effect on the upregulation and expression of ICAM-1 and VCAM-1 (data not shown). Similar results were obtained by using Western immunoblot assay (Fig. 1, *E* and *F*).

CBD attenuates HG-induced increased monocyte adhesion to the endothelial cells

The representative fields containing monocytes adhered to the endothelial cells with the indicated treatments are shown in Fig. 2*A*. HG treatment of HCAECs resulted in a ~4.5-fold increase in monocyte adhesion when compared with normal glucose-treated cells (Fig. 2*B*). Pretreatment of HCAECs with CBD (4 μM) significantly inhibited HG-induced monocyte adhesion to endothelial cells (Fig. 2, *A* and *B*), which was not preventable by CB_1/CB_2 antagonists.

CBD decreases HG-induced monocyte TEM

HG treatment resulted in a marked increase in the monocyte TEM ~3.5 fold when compared with normal glucose-treated cells (Fig. 3). When HCAECs were pretreated with CBD, it significantly reduced the HG-induced increased monocyte TEM, an effect not preventable by either CB_1 or CB_2 antagonists. CB_1 or CB_2 antagonists had no effect on HG-induced TEM by themselves.

CBD attenuates HG-induced disruption of the endothelial barrier function of HCAECs in vitro

HG induced a marked loss of VE-cadherin staining, which was attenuated by CBD pretreatment (Fig. 4*A*). HG treatment resulted in increased endothelial permeability, characterized by increased seepage of dextran-FITC (40 kDa), which was attenuated by CBD pretreatment, an effect not preventable by either CB_1 or CB_2 antagonists (Fig. 4*B*). CB_1 or CB_2 antagonists had no effect on HG-induced disruption of endothelial barrier function by themselves.

CBD moderately attenuates mitochondrial superoxide generation by HG in HCAECs in vitro

HG treatment but not 30 mM D-mannitol (not shown) markedly enhanced mitochondrial superoxide generation (by 3.5-fold) compared with normal glucose in HCAECs. CBD (4 μM) pretreatment attenuated the HG-induced superoxide generation by 23% (Fig. 4*C*).

CBD attenuates HG-induced increased NF-κB activation in HCAECs

Treatment of HCAECs with HG led to marked degradation of IκB-α (cytoplasm; Fig. 5*A*) and increased translocation of NF-κB (p65) to the nucleus (Fig. 5, *B* and *C*). CBD pretreatment largely prevented NF-κB activation, an effect not preventable by either CB_1 or CB_2 antagonists.

CBD attenuates HG-induced increased iNOS expression and 3-NT formation

HG treatment of HCAECs resulted in significant increase in the iNOS expression (~3.5 fold) (Fig. 6, *A* and *B*) and 3-NT formation (Fig. 6*C*) when compared with normal glucose-treated cells. All these phenotypic changes induced by HG were inhibited by CBD.

DISCUSSION

In the present study, we have evaluated the effects of CBD, a nonpsychoactive component of marijuana, on HG-induced mitochondrial superoxide generation, NF-κB activation, iNOS expression, nitrotyrosine formation, upregulation of adhesion molecules ICAM-1 and VCAM-1, monocyte-endothelial adhesion, TEM of monocytes, and disruption of endothelial barrier function in HCAECs. We demonstrate that CBD attenuates HG-induced mitochondrial superoxide generation, NF-κB activation, nitrotyrosine formation, upregulation of iNOS and adhesion molecules ICAM-1 and VCAM-1, TEM of monocytes, monocyte-endothelial adhesion, and disruption of the endothelial barrier function in HCAECs by a mechanism independent from CB_1 and CB_2 receptors.

Consistently, CBD has been shown to exert anti-inflammatory and antioxidant effects both in vitro and in various preclinical models of neurodegeneration and inflammatory disorders, independent from classical CB_1 and CB_2 receptors (6,8,14,19,20,22,25,31,37,46,53). CBD is devoid of psychoactive effects due to a low affinity for the central nervous system CB_1 receptors (37,53) and is well tolerated when chronically administered to humans (7,11). CBD has been approved for the treatment of inflammation, pain, and spasticity associated with multiple sclerosis in humans since 2005 (1,37). Furthermore, CBD has recently been reported to lower the incidence of diabetes in nonobese diabetic mice (55) and to preserve the blood-retinal barrier in experimental diabetes (12).

Numerous epidemiological studies have identified diabetes mellitus as a major risk factor for atherosclerotic cardiovascular diseases such as stroke and coronary heart disease (26). Hyperglycemia triggers the activation of numerous key mechanisms/pathways, such as reactive oxygen species (5) and reactive nitrogen species (40,41), poly(ADP-ribose) polymerase (3, 36,39,42,51), protein kinase C (24), advanced glycation end products (4), and aldose reductase (23,35), eventually leading to endothelial dysfunction in diabetic blood vessels underlying the development of various diabetic complications.

Superoxide production plays a significant role in the pathogenesis of the diabetes-associated endothelial dysfunction (5,18,34,47). The cellular sources of superoxide anion are multiple and include NADH/NADPH and xanthine oxidases, the mitochondrial respiratory chain, the arachidonic acid cascade (including lipoxygenase and cycloxygenase), and microsomal enzymes (5,18,34,47). Among these pathways, mitochondrial generation of superoxide appears to play the most crucial role in diabetic complications (34). Superoxide can also be converted to hydrogen peroxide (H_2O_2) by superoxide dismutase (SOD), and previous studies have suggested that H_2O_2 plays a central role in NF-κB activation in coronary artery endothelial cells (9,10). Hyperglycemia-induced superoxide generation might also favor increased expression of iNOSs through the activation of NF-κB, which increases the generation of nitric oxide. Superoxide anion interacts with nitric oxide, forming the potent cytotoxin peroxynitrite, which attacks various biomolecules in the vascular endothelium, vascular smooth muscle, and myocardium, leading to cardiovascular dysfunction via multiple mechanisms (38,41). The pathogenetic role of nitrosative stress and peroxynitrite and downstream mechanisms is not limited to the diabetes-induced cardiovascular dysfunction but also contributes to the development and progression of diabetic nephropathy, retinopathy, and neuropathy in both experimental animals and humans (38,41).

An increased adhesion of leukocytes (especially monocytes) to the endothelium followed by transmigration into the subendothelial space is a crucial early event in the pathogenesis of atherosclerosis and certain inflammatory disorders [e.g., inflammatory vascular diseases (16, 17)]. HG concentration increases the surface expression of adhesion molecules ICAM-1 and VCAM-1 in endothelial cells, adhesion of endothelial cells to monocytes, and TEM of monocytes in vitro, phenomena related to increased reactive oxygen species generation and NF-κB activation (13,21,27,32,49,52). Studies have also demonstrated increased leukocyte-endothelial interactions with monocytes from diabetic patients (16,29) and in animal models of diabetes (16,54). Recently, Li et al. (30) have reported that macrophages and vascular smooth muscle cells isolated from diabetic mice exhibited proatherogenic properties, such as enhanced adhesion and migration that were largely dependent on NF-κB activation (30).

Consistent with these previous reports, we found that HG increased mitochondrial superoxide generation, 3-NT formation, NF-κB activation, upregulation of iNOS and adhesion molecules ICAM-1 and VCAM-1, TEM of monocytes, and monocyte-endothelial adhesion in HCAECs (Fig. 6*D*). HG also decreased endothelial barrier function measured by increased permeability and diminished expression of VE-cadherin in HCAECs (Fig. 6*D*). Remarkably, all the above-mentioned effects of HG were attenuated by CBD (Fig. 6*D*). Since reactive oxygen species/peroxynitrite/NF-κB pathway and downstream effectors, such as poly(ADP-ribose) polymerase-1, play important roles in the destruction of insulin-secreting pancreatic β-cells (reviewed in Ref. 38), it is conceivable that the above-mentioned anti-inflammatory effects of CBD could contribute to the recently observed antidiabetic effects in nonobese diabetic mice (55).

Collectively, our results suggest that the nonpsychoactive cannabinoid CBD have significant therapeutic benefits against diabetic complications and atherosclerosis by attenuating HG-induced mitochondrial superoxide generation, increased NF-κB activation, upregulation of iNOS and adhesion molecules, 3-NT formation, monocyte-endothelial adhesion, TEM of monocytes, and disruption of the endothelial barrier function. This is particularly encouraging in light of the excellent safety and tolerability profile of CBD in humans.

Acknowledgements

We are indebted to Prof. Raphael Mechoulam for providing cannabidiol and valuable comments on the manuscript.

GRANTS

This study was supported by the National Institute on Alcohol Abuse and Alcoholism Intramural Research Program (to P. Pacher).

References

1. Barnes MP. Sativex: clinical efficacy and tolerability in the treatment of symptoms of multiple sclerosis and neuropathic pain. Expert Opin Pharmacother 2006;7:607–615. [PubMed: 16553576]
2. Bhunia AK, Arai T, Bulkley G, Chatterjee S. Lactosylceramide mediates tumor necrosis factor-alpha-induced intercellular adhesion molecule-1 (ICAM-1) expression and the adhesion of neutrophil in human umbilical vein endothelial cells. J Biol Chem 1998;273:34349–34357. [PubMed: 9852101]
3. Brownlee M. The pathobiology of diabetic complications: a unifying mechanism. Diabetes 2005;54:1615–1625. [PubMed: 15919781]
4. Brownlee M, Cerami A, Vlassara H. Advanced glycosylation end products in tissue and the biochemical basis of diabetic complications. N Engl J Med 1988;318:1315–1321. [PubMed: 3283558]
5. Ceriello A. Oxidative stress and diabetes-associated complications. Endocr Pract 2006;12(Suppl 1): 60–62. [PubMed: 16627383]
6. Chen Y, Buck J. Cannabinoids protect cells from oxidative cell death: a receptor-independent mechanism. J Pharmacol Exp Ther 2000;293:807–812. [PubMed: 10869379]
7. Consroe P, Laguna J, Allender J, Snider S, Stern L, Sandyk R, Kennedy K, Schram K. Controlled clinical trial of cannabidiol in Huntington's disease. Pharmacol Biochem Behav 1991;40:701–708. [PubMed: 1839644]
8. Costa B, Colleoni M, Conti S, Parolaro D, Franke C, Trovato AE, Giagnoni G. Oral anti-inflammatory activity of cannabidiol, a non-psychoactive constituent of cannabis, in acute carrageenan-induced inflammation in the rat paw. Naunyn Schmiedebergs Arch Pharmacol 2004;369:294–299. [PubMed: 14963641]
9. Csiszar A, Ahmad M, Smith KE, Labinskyy N, Gao Q, Kaley G, Edwards JG, Wolin MS, Ungvari Z. Bone morphogenetic protein-2 induces proinflammatory endothelial phenotype. Am J Pathol 2006;168:629–638. [PubMed: 16436676]
10. Csiszar A, Smith K, Labinskyy N, Orosz Z, Rivera A, Ungvari Z. Resveratrol attenuates TNF-alpha-induced activation of coronary arterial endothelial cells: role of NF-kappaB inhibition. Am J Physiol Heart Circ Physiol 2006;291:H1694–H1699. [PubMed: 16973825]
11. Cunha JM, Carlini EA, Pereira AE, Ramos OL, Pimentel C, Gagliardi R, Sanvito WL, Lander N, Mechoulam R. Chronic administration of cannabidiol to healthy volunteers and epileptic patients. Pharmacology 1980;21:175–185. [PubMed: 7413719]
12. El-Remessy AB, Al-Shabrawey M, Khalifa Y, Tsai NT, Caldwell RB, Liou GI. Neuroprotective and blood-retinal barrier-preserving effects of cannabidiol in experimental diabetes. Am J Pathol 2006;168:235–244. [PubMed: 16400026]
13. Esposito C, Fasoli G, Plati AR, Bellotti N, Conte MM, Cornacchia F, Foschi A, Mazzullo T, Semeraro L, Dal Canton A. Long-term exposure to high glucose up-regulates VCAM-induced endothelial cell adhesiveness to PBMC. Kidney Int 2001;59:1842–1849. [PubMed: 11318955]
14. Esposito G, De Filippis D, Maiuri MC, De Stefano D, Carnuccio R, Iuvone T. Cannabidiol inhibits inducible nitric oxide synthase protein expression and nitric oxide production in beta-amyloid stimulated PC12 neurons through p38 MAP kinase and NF-kappaB involvement. Neurosci Lett 2006;399:91–95. [PubMed: 16490313]
15. Gaoni Y, Mechoulam R. The isolation and structure of delta-1-tetrahydrocannabinol and other neutral cannabinoids from hashish. J Am Chem Soc 1971;93:217–224. [PubMed: 5538858]
16. Gerrity RG. The role of the monocyte in atherogenesis: I. Transition of blood-borne monocytes into foam cells in fatty lesions. Am J Pathol 1981;103:181–190. [PubMed: 7234961]
17. Gerrity RG. The role of the monocyte in atherogenesis: II. Migration of foam cells from atherosclerotic lesions. Am J Pathol 1981;103:191–200. [PubMed: 7234962]
18. Guzik TJ, Mussa S, Gastaldi D, Sadowski J, Ratnatunga C, Pillai R, Channon KM. Mechanisms of increased vascular superoxide production in human diabetes mellitus: role of NAD(P)H oxidase and endothelial nitric oxide synthase. Circulation 2002;105:1656–1662. [PubMed: 11940543]

19. Hamelink C, Hampson A, Wink DA, Eiden LE, Eskay RL. Comparison of cannabidiol, antioxidants, and diuretics in reversing binge ethanol-induced neurotoxicity. J Pharmacol Exp Ther 2005;314:780–788. [PubMed: 15878999]
20. Hampson AJ, Grimaldi M, Axelrod J, Wink D. Cannabidiol and (−)delta9-tetrahydrocannabinol are neuroprotective antioxidants. Proc Natl Acad Sci USA 1998;95:8268–8273. [PubMed: 9653176]
21. Hamuro M, Polan J, Natarajan M, Mohan S. High glucose induced nuclear factor kappa B mediated inhibition of endothelial cell migration. Atherosclerosis 2002;162:277–287. [PubMed: 11996947]
22. Hayakawa K, Mishima K, Abe K, Hasebe N, Takamatsu F, Yasuda H, Ikeda T, Inui K, Egashira N, Iwasaki K, Fujiwara M. Cannabidiol prevents infarction via the non-CB1 cannabinoid receptor mechanism. Neuroreport 2004;15:2381–2385. [PubMed: 15640760]
23. Hotta N. New approaches for treatment in diabetes: aldose reductase inhibitors. Biomed Pharmacother 1995;49:232–243. [PubMed: 7579002]
24. Ishii H, Koya D, King GL. Protein kinase C activation and its role in the development of vascular complications in diabetes mellitus. J Mol Med 1998;76:21–31. [PubMed: 9462865]
25. Iuvone T, Esposito G, Esposito R, Santamaria R, Di Rosa M, Izzo AA. Neuroprotective effect of cannabidiol, a non-psychoactive component from Cannabis sativa, on beta-amyloid-induced toxicity in PC12 cells. J Neurochem 2004;89:134–141. [PubMed: 15030397]
26. Kannel WB, McGee DL. Diabetes and cardiovascular risk factors: the Framingham study. Circulation 1979;59:8–13. [PubMed: 758126]
27. Kim JA, Berliner JA, Natarajan RD, Nadler JL. Evidence that glucose increases monocyte binding to human aortic endothelial cells. Diabetes 1994;43:1103–1107. [PubMed: 7520876]
28. Klein TW. Cannabinoid-based drugs as anti-inflammatory therapeutics. Nat Rev Immunol 2005;5:400–411. [PubMed: 15864274]
29. Kunt T, Forst T, Fruh B, Flohr T, Schneider S, Harzer O, Pfutzner A, Engelbach M, Lobig M, Beyer J. Binding of monocytes from normolipidemic hyperglycemic patients with type 1 diabetes to endothelial cells is increased in vitro. Exp Clin Endocrinol Diabetes 1999;107:252–256. [PubMed: 10433064]
30. Li SL, Reddy MA, Cai Q, Meng L, Yuan H, Lanting L, Natarajan R. Enhanced proatherogenic responses in macrophages and vascular smooth muscle cells derived from diabetic db/db mice. Diabetes 2006;55:2611–2619. [PubMed: 16936211]
31. Malfait AM, Gallily R, Sumariwalla PF, Malik AS, Andreakos E, Mechoulam R, Feldmann M. The nonpsychoactive cannabis constituent cannabidiol is an oral anti-arthritic therapeutic in murine collagen-induced arthritis. Proc Natl Acad Sci USA 2000;97:9561–9566. [PubMed: 10920191]
32. Morigi M, Angioletti S, Imberti B, Donadelli R, Micheletti G, Figliuzzi M, Remuzzi A, Zoja C, Remuzzi G. Leukocyte-endothelial interaction is augmented by high glucose concentrations and hyperglycemia in a NF-kB-dependent fashion. J Clin Invest 1998;101:1905–1915. [PubMed: 9576755]
33. Nakagami H, Morishita R, Yamamoto K, Yoshimura SI, Taniyama Y, Aoki M, Matsubara H, Kim S, Kaneda Y, Ogihara T. Phosphorylation of p38 mitogen-activated protein kinase downstream of bax-caspase-3 pathway leads to cell death induced by high D-glucose in human endothelial cells. Diabetes 2001;50:1472–1481. [PubMed: 11375350]
34. Nishikawa T, Edelstein D, Du XL, Yamagishi S, Matsumura T, Kaneda Y, Yorek MA, Beebe D, Oates PJ, Hammes HP, Giardino I, Brownlee M. Normalizing mitochondrial superoxide production blocks three pathways of hyperglycaemic damage. Nature 2000;404:787–790. [PubMed: 10783895]
35. Obrosova IG. Increased sorbitol pathway activity generates oxidative stress in tissue sites for diabetic complications. Antioxid Redox Signal 2005;7:1543–1552. [PubMed: 16356118]
36. Obrosova IG, Julius UA. Role for poly(ADP-ribose) polymerase activation in diabetic nephropathy, neuropathy and retinopathy. Curr Vasc Pharmacol 2005;3:267–283. [PubMed: 16026323]
37. Pacher P, Batkai S, Kunos G. The endocannabinoid system as an emerging target of pharmacotherapy. Pharmacol Rev 2006;58:389–462. [PubMed: 16968947]
38. Pacher P, Beckman J, Liaudet L. Nitric oxide and peroxynitrite in health and disease. Physiol Rev 2007;87:315–424. [PubMed: 17237348]

39. Pacher P, Liaudet L, Soriano FG, Mabley JG, Szabo E, Szabo C. The role of poly(ADP-ribose) polymerase activation in the development of myocardial and endothelial dysfunction in diabetes. Diabetes 2002;51:514–521. [PubMed: 11812763]
40. Pacher P, Obrosova IG, Mabley JG, Szabo C. Role of nitrosative stress and peroxynitrite in the pathogenesis of diabetic complications. Emerging new therapeutical strategies. Curr Med Chem 2005;12:267–275. [PubMed: 15723618]
41. Pacher P, Szabo C. Role of peroxynitrite in the pathogenesis of cardiovascular complications of diabetes. Curr Opin Pharmacol 2006;6:136–141. [PubMed: 16483848]
42. Pacher P, Szabo C. Role of poly(ADP-ribose) polymerase-1 activation in the pathogenesis of diabetic complications: endothelial dysfunction, as a common underlying theme. Antioxid Redox Signal 2005;7:1568–1580. [PubMed: 16356120]
43. Piacenza L, Irigoin F, Alvarez MN, Peluffo G, Taylor MC, Kelly JM, Wilkinson SR, Radi R. Mitochondrial superoxide radicals mediate programmed cell death in Trypanosoma cruzi: cytoprotective action of mitochondrial Fe-superoxide dismutase overexpression. Biochem J 2007;403:323–334. [PubMed: 17168856]
44. Rattan V, Shen Y, Sultana C, Kumar D, Kalra VK. Glucose-induced transmigration of monocytes is linked to phosphorylation of PECAM-1 in cultured endothelial cells. Am J Physiol Endocrinol Metab 1996;271:E711–E717.
45. Robinson KM, Janes MS, Pehar M, Monette JS, Ross MF, Hagen TM, Murphy MP, Beckman JS. Selective fluorescent imaging of superoxide in vivo using ethidium-based probes. Proc Natl Acad Sci USA 2006;103:15038–15043. [PubMed: 17015830]
46. Sacerdote P, Martucci C, Vaccani A, Bariselli F, Panerai AE, Colombo A, Parolaro D, Massi P. The nonpsychoactive component of marijuana cannabidiol modulates chemotaxis and IL-10 and IL-12 production of murine macrophages both in vivo and in vitro. J Neuroimmunol 2005;159:97–105. [PubMed: 15652407]
47. San Martin A, Du P, Dikalova A, Lassegue B, Aleman M, Gongora MC, Brown K, Joseph G, Harrison DG, Taylor WR, Jo H, Griendling KK. Reactive oxygen species-selective regulation of aortic inflammatory gene expression in Type 2 diabetes. Am J Physiol Heart Circ Physiol 2007;292:H2073–H2082. [PubMed: 17237245]
48. Sanchez T, Estrada-Hernandez T, Paik JH, Wu MT, Venkataraman K, Brinkmann V, Claffey K, Hla T. Phosphorylation and action of the immunomodulator FTY720 inhibits vascular endothelial cell growth factor-induced vascular permeability. J Biol Chem 2003;278:47281–47290. [PubMed: 12954648]
49. Shanmugam N, Reddy MA, Guha M, Natarajan R. High glucose-induced expression of proinflammatory cytokine and chemokine genes in monocytic cells. Diabetes 2003;52:1256–1264. [PubMed: 12716761]
50. Stevens MJ. Oxidative-nitrosative stress as a contributing factor to cardiovascular disease in subjects with diabetes. Curr Vasc Pharmacol 2005;3:253–266. [PubMed: 16026322]
51. Szabo C, Zanchi A, Komjati K, Pacher P, Krolewski AS, Quist WC, LoGerfo FW, Horton ES, Veves A. Poly(ADP-ribose) polymerase is activated in subjects at risk of developing Type 2 diabetes and is associated with impaired vascular reactivity. Circulation 2002;106:2680–2686. [PubMed: 12438293]
52. Takami S, Yamashita S, Kihara S, Kameda-Takemura K, Matsuzawa Y. High concentration of glucose induces the expression of intercellular adhesion molecule-1 in human umbilical vein endothelial cells. Atherosclerosis 1998;138:35–41. [PubMed: 9678769]
53. Thomas BF, Gilliam AF, Burch DF, Roche MJ, Seltzman HH. Comparative receptor binding analyses of cannabinoid agonists and antagonists. J Pharmacol Exp Ther 1998;285:285–292. [PubMed: 9536023]
54. Tsao PS, Niebauer J, Buitrago R, Lin PS, Wang BY, Cooke JP, Chen YD, Reaven GM. Interaction of diabetes and hypertension on determinants of endothelial adhesiveness. Arterioscler Thromb Vasc Biol 1998;18:947–953. [PubMed: 9633936]
55. Weiss L, Zeira M, Reich S, Har-Noy M, Mechoulam R, Slavin S, Gallily R. Cannabidiol lowers incidence of diabetes in non-obese diabetic mice. Autoimmunity 2006;39:143–151. [PubMed: 16698671]

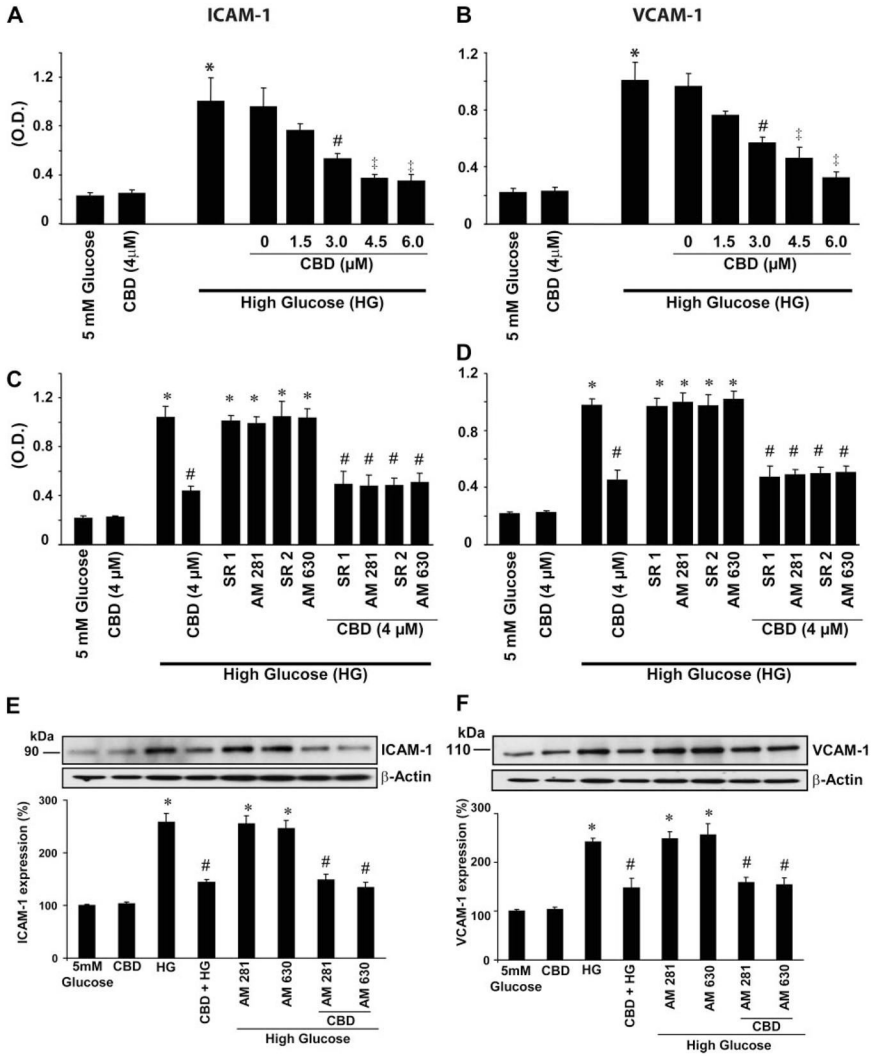

Fig. 1.

Effect of cannabidiol (CBD) on high glucose (HG)-induced increased ICAM-1 and VCAM-1 expressions in human coronary artery endothelial cells (HCAECs). Cells were treated with either normal glucose (5 mM) or HG (30 mM) alone for 48 h or pretreated with CBD at indicated concentrations followed by treatment with HG for 48 h, and cell-surface ELISA was then performed by measuring absorbance at 450 nm as described in MATERIALS AND METHODS. *A*: effect of CBD on HG-induced increased ICAM-1 expression. **P* < 0.001 vs. 5 mM glucose; #*P* < 0.001 vs. HG; ‡*P* < 0.05 vs. HG. OD, optical density (*n* = 9). *B*: effect of CBD on HG-induced increased VCAM-1 expression. **P* < 0.001 vs. 5 mM glucose; #*P* < 0.001 vs. HG; ‡*P* < 0.05 vs. HG (*n* = 9). Cells were treated with either normal glucose, HG, or CBD alone for 48 h or pretreated with either cannabinoid-1 or -2 (CB_1 or CB_2, respectively) antagonists (1 μM each) followed by treatment with either HG alone or in combination with CBD, and cell surface ELISA was performed for ICAM-1 (*C*) or VCAM-1 (*D*) expression (*n* = 9). **P* < 0.0001 vs. normal glucose; #*P* < 0.001 vs. HG (*n* = 3). *E*: representative ICAM-1 immunoblot from 3 identical blots depicting the effect of indicated treatments on ICAM-1 expression. **P* < 0.001 vs. 5 mM glucose or CBD (4 μM alone); #*P* < 0.01 vs. HG. *F*: representative VCAM-1 immunoblot from 3 identical blots depicting the effect of indicated

treatments on VCAM-1 expression. *$P < 0.01$ vs. 5mM glucose or CBD (4 μM alone); #$P < 0.01$ vs. HG ($n = 3$).

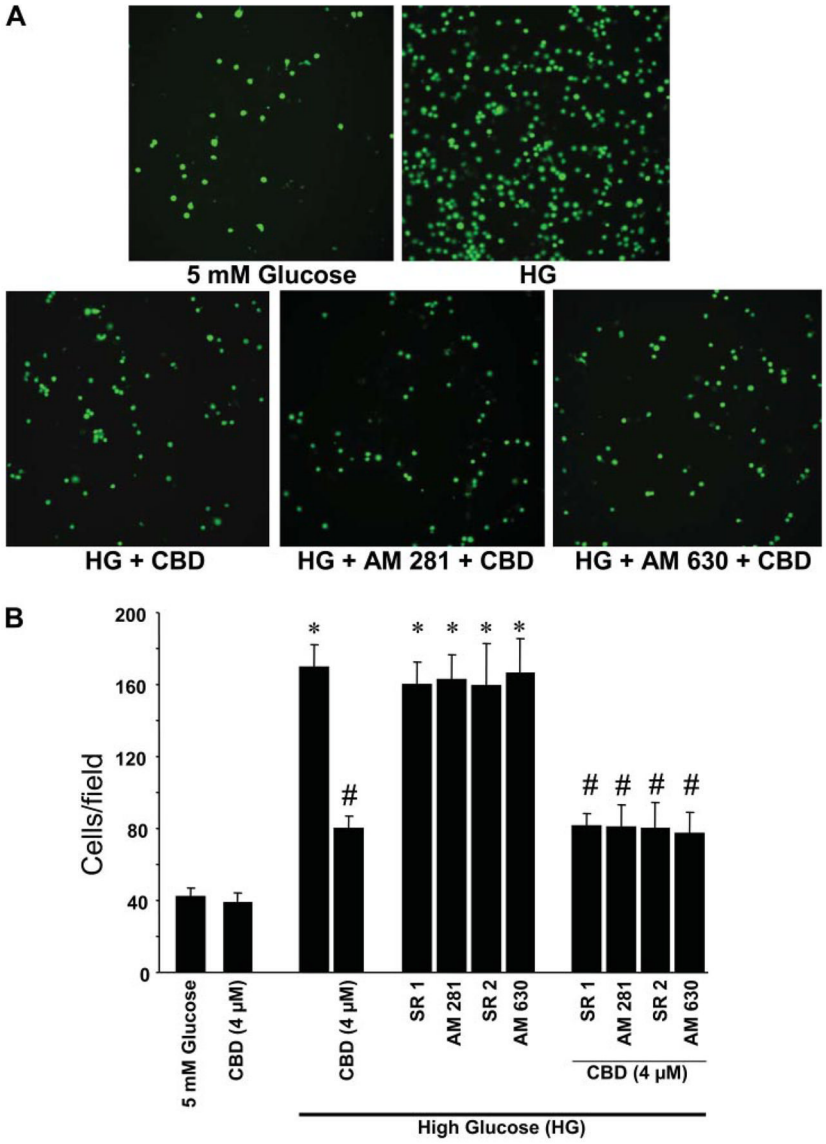

Fig. 2.

Effect of CBD on HG-induced increased monocyte adhesion to endothelial cells. *A*: representative pictures of monocytes adhered to HCAECs. HCAECs were either treated with normal glucose, HG for 48 h, or pretreated with CBD (4 μM) or either CB_1 or CB_2 antagonists followed by incubation with HG alone or in combination with CBD, and adhesion assays were performed as described in the MATERIALS AND METHODS. *B*: quantification data for monocyte adhered to endothelial cells from 3 independent experiments. *$P < 0.001$ vs. normal glucose; #$P < 0.001$ vs. HG.

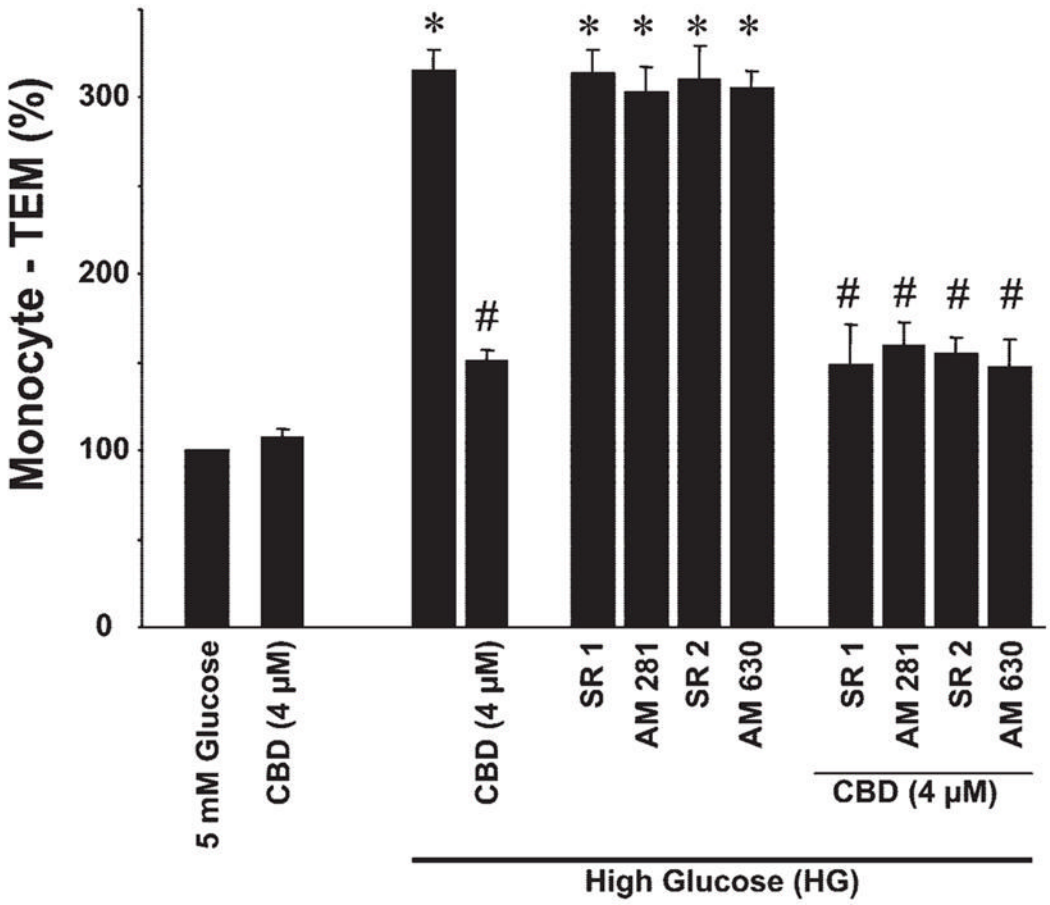

Fig. 3.

Effect of CBD on HG-induced increased monocyte transendothelial migration (TEM). HCAECs were treated with either normal glucose, HG, or CBD for 48 h or pretreated with CBD or either CB_1 or CB_2 antagonists followed by incubation with HG ± CBD and continued incubation for 48 h, and monocyte adhesion TEM assays were performed as outlined in MATERIALS AND METHODS. *$P < 0.001$ vs. control or normal glucose; #$P < 0.001$ vs. HG ($n = 6$).

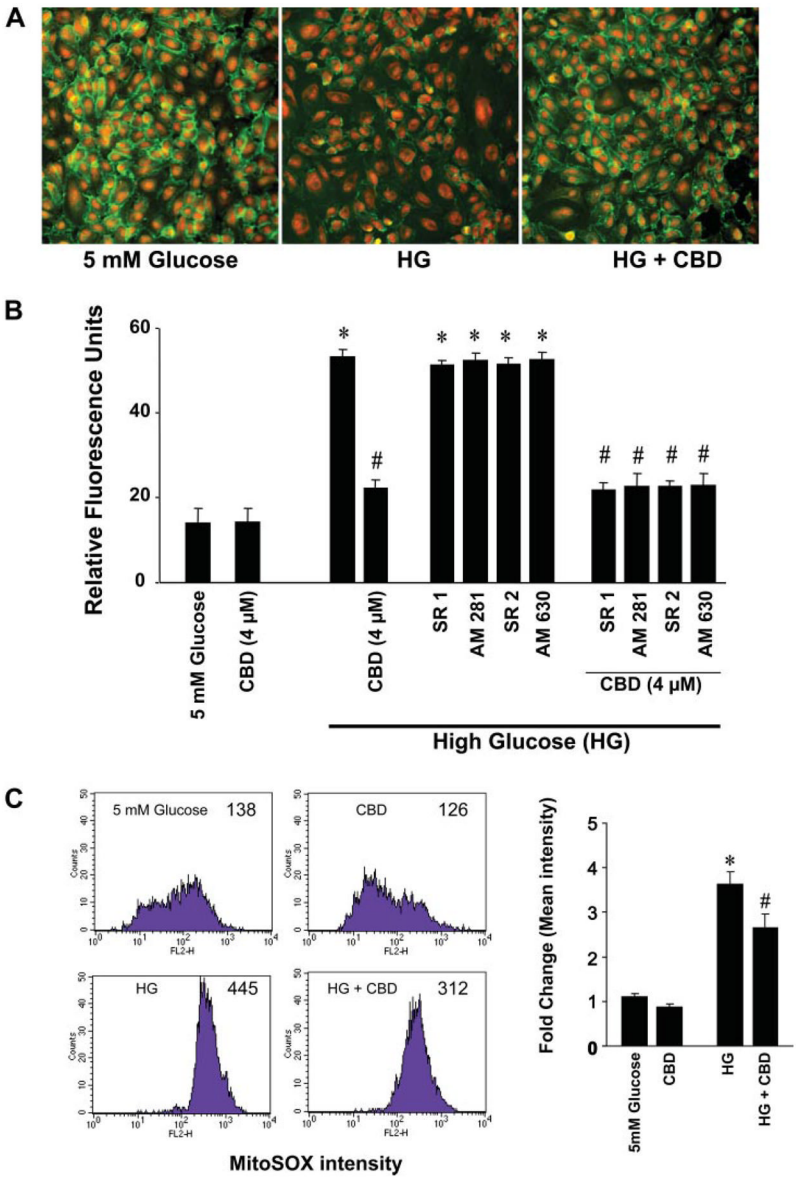

Fig. 4.

Effect of CBD on HG-induced barrier dysfunction and mitochondrial superoxide production. *A*: representative images of immunofluorescence staining for vascular endothelial cadherin expression in HCAECs from 3 independent experiments with similar results. *B*: quantitative data for in vitro transcellular hyperpermeability of FITC-dextran induced by HG and the effect of CBD on HG-induced barrier dysfunction in HCAECs. **P* < 0.001 vs. normal glucose; #*P* < 0.001 vs. HG (*n* = 6). *C*: effect of CBD on HG induced mitochondrial superoxide production. Mitocondrial superoxide generation was then determined by FACS calibur system using MitoSOX as described in MATERIALS AND METHODS.Shown are representative flow cytometry data of mitochondrial superoxide formation by HG and partial attenuation CBD. Quantifications were performed from mean intensity of MitoSOX fluorescence from 3 independent experiments. Error bars represent standard deviation. *C*, *left*: numbers in graphs represent mean fluorescence intensity. **P* < 0.001 vs. normal glucose; #*P* < 0.05 vs. HG (*n* = 3).

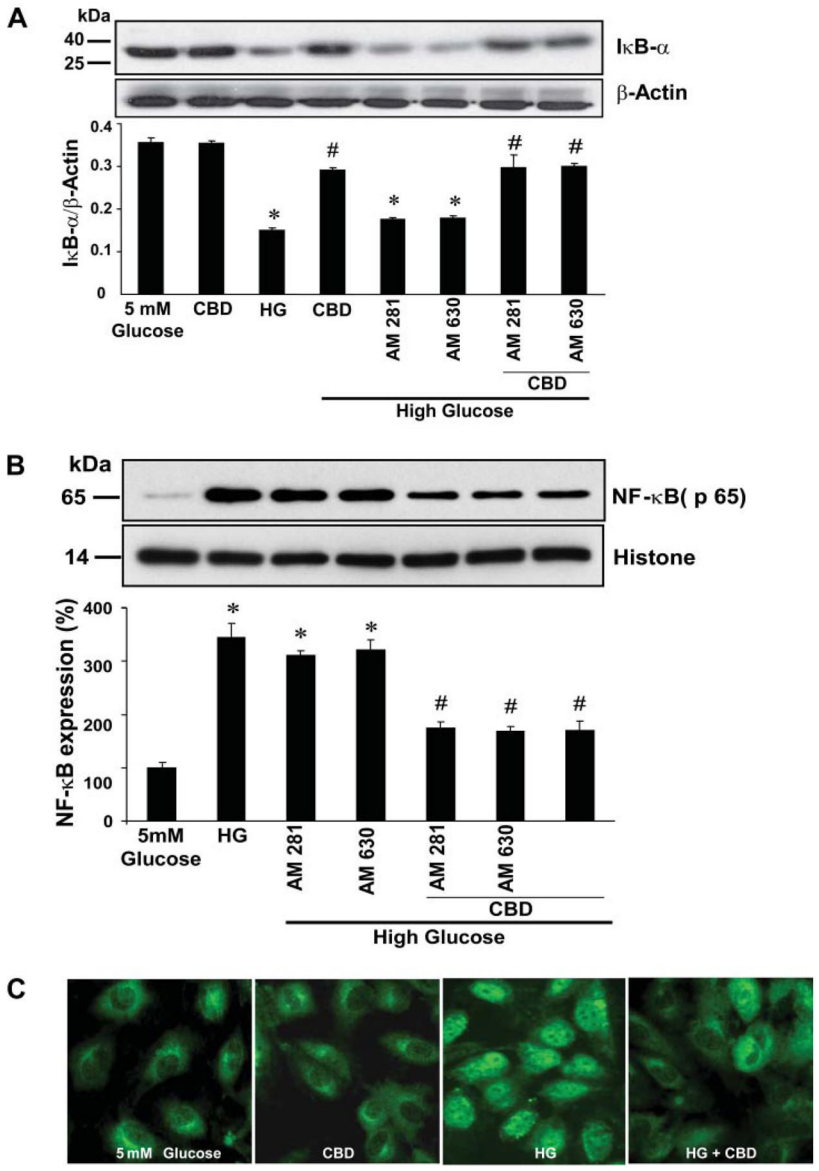

Fig. 5.

Effect of CBD on HG-induced NF-κB activation. *A, top*: HCAECs were treated as indicated, cytoplasmic extracts were prepared, and Western immunoblot assays were performed to determine inhibitory κB-α factor (IκB-α) degradation. Shown is the representative blot from 3 independent experiments with similar results. *A, bottom*: quantification of IκB-α degradation in the cytosol. **P* < 0.001 vs. control; #*P* < 0.001 vs. HG. *B, top*: representative blot for NF-κB (p65) expression in nuclear extracts prepared after treatments as indicated. *B, bottom*: quantification data for NF-κB expression in nucleus after normalization with histone. **P* < 0.01 vs. control; #*P* < 0.01 vs. HG (*n* = 3). *C*: HG-induced nuclear translocation of NF-κB (p65), indicating its activation and its inhibition by CBD. Note intense nuclear staining of p65 in HG-treated cells. Shown are representative images from 5 independent experiments yielding similar results.

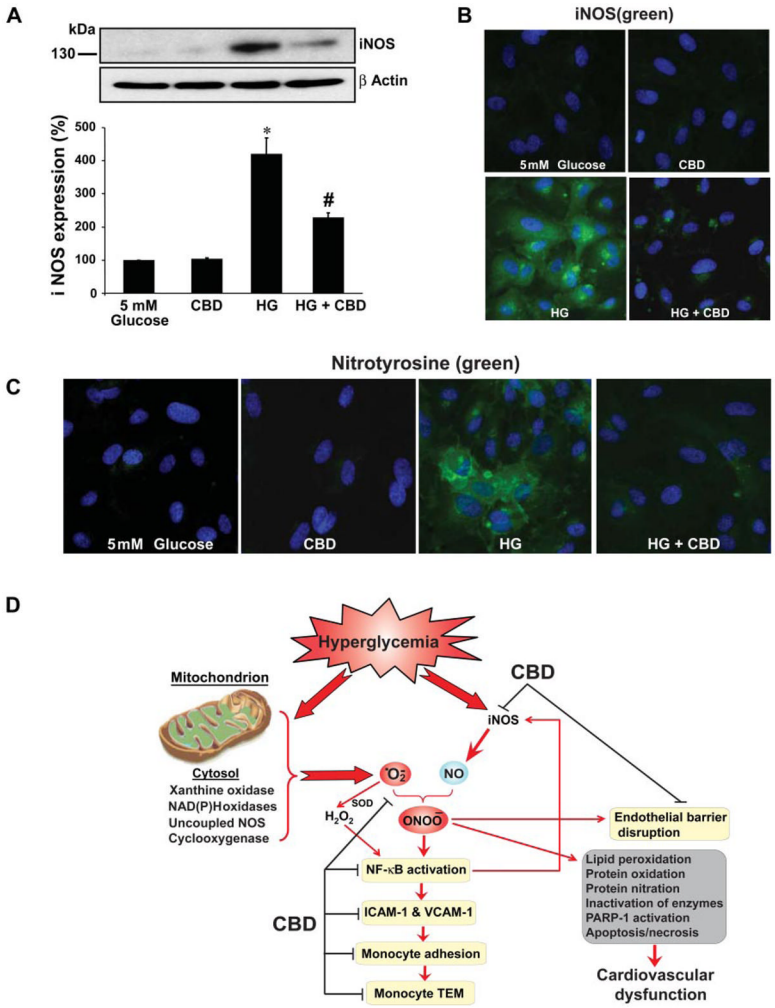

Fig. 6.

Effect of CBD on HG-induced inducible nitric oxide (NO) synthase (iNOS) expression and 3-nitrotyrosine (3-NT) formation, proposed protective mechanisms of CBD. *A*: HCAECs were treated with either normal glucose, CBD (4 μM), HG alone for 48 h or pretreated with CBD followed by HG treatment for 48 h. Total cell lysates were prepared, and 25 μg of protein were resolved on 12% SDS-PAGE gels and probed with anti-human iNOS (monoclonal, used at 1:1,000 dilution; BD Biosciences). Shown is the representative image from 3 separate experiments with identical results. **P* < 0.001 vs. 5 mM glucose; #*P* < 0.01 vs. HG. *B*: HCAECs were treated as described above, and iNOS expression was analyzed by immunofluorescene staining (mouse monoclonal anti-human iNOS at 1:150 dilution). The nuclei were counterstained with 4′,6-diamidino-2-phenylindole dihydrochloride (DAPI; Molecular Probes, Invitrogen). Shown are representative images from 3 separate experiments. *C*: 3-NT formation in HG-treated cells and effects of CBD by immunofluorescence assay. Nuclei were counterstained with DAPI. Shown are images from 3 independent experiments with identical results. *D*: proposed protective mechanisms of CBD against HG-induced endothelial cell inflammatory response and barrier disruption. Mitochondrion is considered to be the major source of hyperglycemia-induced increased superoxide anion production; however, other sources such as xanthine and NAD(P)H oxidases, cyclooxygenase, and uncoupled NOS may also contribute to this process under certain conditions. Hyperglycemia-induced superoxide generation might also favor increased expression of iNOS through activation of NF-κB, which

increases the generation of NO. Superoxide anion quenches NO, thereby reducing the efficacy of a potent endothelium-derived vasodilator system. Superoxide can also be converted to hydrogen peroxide by SOD and interact with NO to form a reactive oxidant peroxynitrite (ONOO–), which induces cell damage via lipid peroxidation, inactivation of enzymes and other proteins by oxidation and nitration, and activation of nuclear enzyme poly(ADP-ribose) polymerase (PARP-1). Red arrows/lines indicate activation, and black lines indicate inhibition.